Ecological Engineering 84 (2015) 476–484

Contents lists available at ScienceDirect

Ecological Engineering

journal homepage: www.elsevier.com/locate/ecoleng

Extensive field measurements of flow in vertical slot fishway as data for validation of numerical simulations

Martin Bombač[a,*], Gorazd Novak[a], Jurij Mlačnik[a], Matjaž Četina[b]

[a] Institute for Hydraulic Research, Hajdrihova 28, Ljubljana, Slovenia
[b] University of Ljubljana, Faculty of Civil and Geodetic Engineering, Chair of Fluid Mechanics with Laboratory, Hajdrihova 28, Ljubljana, Slovenia

ARTICLE INFO

Article history:
Received 17 March 2015
Received in revised form 15 July 2015
Accepted 4 September 2015

Keywords:
Vertical slot fishway
Field measurements
Numerical simulations
Two-dimensional depth-averaged model
Hydraulic model
Velocity field

ABSTRACT

Fishways are of great ecological importance and have been the focus of numerous studies. However, many fishways remain operating at an unsatisfactory level. Furthermore, field measurements of flow properties in effective fishways remain surprisingly rare compared to the number of various numerical and physical hydraulic models. The purpose of the research was to conduct extensive field measurements of the flow in an effectively operating vertical slot fishway (VSF), and to use the findings to calibrate and verify the depth-averaged two-dimensional (2D) numerical hydraulic model PCFLOW2D. Flow velocities were measured using a reliable 3D acoustic probe. Measured velocities were up to 50% larger than values calculated from an equation proposed in recent literature, but in accordance with results of our simulations. PCFLOW2D proved to be a useful tool for modeling fishway flow and could be used in similar hydro-environmental problems.

1. Introduction

Fish of all ages migrate up and downstream to meet their needs (e.g. feeding, reproduction) which cannot be fulfilled where they are (Katopodis, 1992). Obstructions such as dams can have long-term negative effects on biodiversity and distribution of fish populations. Effective fishways bridge the interruption of fish migration routes and are of great ecological importance.

Different types of technical fishways are known from the literature: weir, Denil, culvert and VSF type. The subject of this paper is the VSF type. This area of research has been the focus of numerous studies (Bermúdez et al., 2010; Cea et al., 2007; Liu et al., 2006; Marriner et al., 2014; Rajaratnam et al., 1986, 1992; Tarrade et al., 2008, 2011). The main advantage of the VSF type is that the hydraulic characteristics in such a fishway are quasi-independent from the discharge or water depth variation in the fishway (Chorda et al., 2010; Katopodis, 1992). Another advantage of this type of fishway is extremely small velocities between the boulders on the bottom of the fishway, enabling the migration of other aquatic organisms.

The fishway related legislation demands certain ecological conditions of watercourses (Water Framework Directive, 2000/60/EC; The Habitat Directive – FFH, 92/43/EEC), but fishways often remain relatively non-functional, as recently shown by Ciuha et al. (2014). Therefore, it is necessary to pay special attention to the design of new and reconstruction of old fishways. For example, according to monitoring on larger dams in Slovenia only one fishway was confirmed as fully functional (Ciuha et al., 2014; Kolman et al., 2010), and this fishway is the subject of the present paper.

The objective of the work is threefold. Firstly, to present results of extensive field measurements of flow depths and velocities in the observed VSF, since such results are still rare but valuable for the calibration and verification of numerical and physical hydraulic models. Secondly, to verify the value of the maximum velocity in the slot, proposed in design manuals by Larinier (2002), Maddock et al. (2013), and in studies by Calluaud et al. (2014), Liu et al. (2006), and Puertas et al. (2004) as the relation $v_{max} = (2g\Delta h)^{1/2}$. Thirdly, to calibrate, verify and evaluate PCFLOW2D hydraulic model as a tool in the process of a VSF design.

2. Material and methods

2.1. Field measurements

The fishway considered in this paper is built at the Arto – Blanca hydropower plant and consists of two reaches: upstream concrete

* Corresponding author.
E-mail addresses: martin.bombac@hidroinstitut.si (M. Bombač), gorazd.novak@hidroinstitut.si (G. Novak), jurij.mlacnik@hidroinstitut.si (J. Mlačnik), matjaz.cetina@fgg.uni-lj.si (M. Četina).

http://dx.doi.org/10.1016/j.ecoleng.2015.09.030
0925-8574/

Nomenclature

Notation

b_0	slot width [m]
d_x	short baffle pier width [m]
d_y	short baffle pier length [m]
E	energy dissipation rate per unit volume [W m^{-3}]
$\bar{E}$	average energy dissipation rate per unit volume [W m^{-3}]
g	gravity acceleration [m s^{-2}]
h	water depth [m]
k	mean flow kinetic energy per unit mass [m^2 s^{-2}]
k'	turbulent kinetic energy per unit mass [m^2 s^{-2}]
L	pool length [m]
n_g	Manning's roughness coefficient [s m$^{-1/3}$]
Q	discharge [m^3/s]
S_0	longitudinal slope [–]
v_{max}	maximum velocity in the slot of a VSF [m/s]
V_p	pool water volume [m^3]
v_x	mean longitudinal velocity component [m/s]
v_y	mean transverse velocity component [m/s]
v_z	mean vertical velocity component [m/s]
W	pool width [m]
x	longitudinal coordinate [m]
y	transverse coordinate [m]
z	vertical coordinate [m]
z_b	bed elevation level [m.a.s.l.]
Δh	head difference between two adjacent pools [m]
Δt	time step [s]
Δx	cell size in longitudinal direction [m]
Δy	cell size in transverse direction [m]
ε	dissipation rate per unit mass [m^2 s^{-3}]
ν_T	kinematic coefficient of eddy viscosity [m^2 s^{-1}]
ρ	water density [kg m^{-3}]
ψ	streamline [m^3/s]
ψ'	dimensionless streamline [–]

reach with 24 vertical slots (i.e. VSF reach), and a much more natural-like downstream reach with meanders. This paper focuses on the VSF reach. Geometry of the observed pool in the VSF is shown in Fig. 1.During field measurements the VSF flow conditions (i.e.

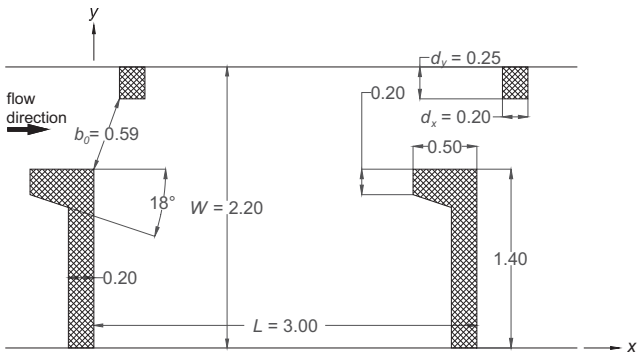

Fig. 1. Details of a pool in the presented VSF. Dimensions are in meters.

inflow, outflow, water surface slope) were kept constant, namely: discharge $Q = 1.00\,m^3/s$, water depth $h = 1.30\,m$, head difference between pools $\Delta h = 0.05\,m$, water surface slope $S_0 = 0.0167$. In the selected pool, located in the middle of the upstream straight concrete reach, the following parameters were measured: water surface elevation, bed elevation, and all three velocity components. Elevations were determined with leveling, while flow velocities were measured with SonTek 3D Micro-Acoustic Doppler Velocimeter (i.e. ADV). The probe was positioned with an adjustable traverse and caused negligible disturbance to the observed flow. The following user-defined settings were used: sampling frequency of 50 Hz, and measuring area of ±2.50 m/s. The suitability of the measurement was confirmed by achieved signal correlation factor $C_{avg} = 86\%$ (with $66 < C < 97$) and signal-to-noise ratio $SNR_{avg} = 22$ dB (with $18 < SNR < 27$). Flow velocities were measured in a total of 254 points located 0.05–0.20 m apart, as shown in Fig. 2.

2.2. Numerical model

Numerical simulations were performed with the PCFLOW2D model. PCFLOW2D solves the depth-averaged shallow water equations coupled with a turbulence model. The 2D depth-averaged shallow water equations can be written in conservative form as:

$$\frac{\partial h}{\partial t} + \frac{\partial (h v_x)}{\partial x} + \frac{\partial (h v_y)}{\partial y} = 0 \quad (1)$$

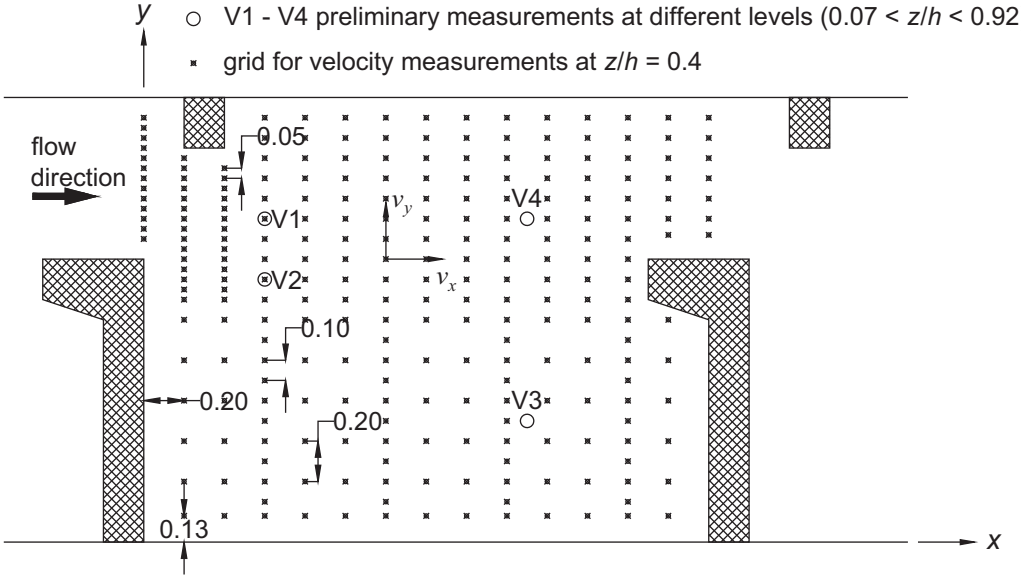

Fig. 2. Locations of flow velocity measurements.

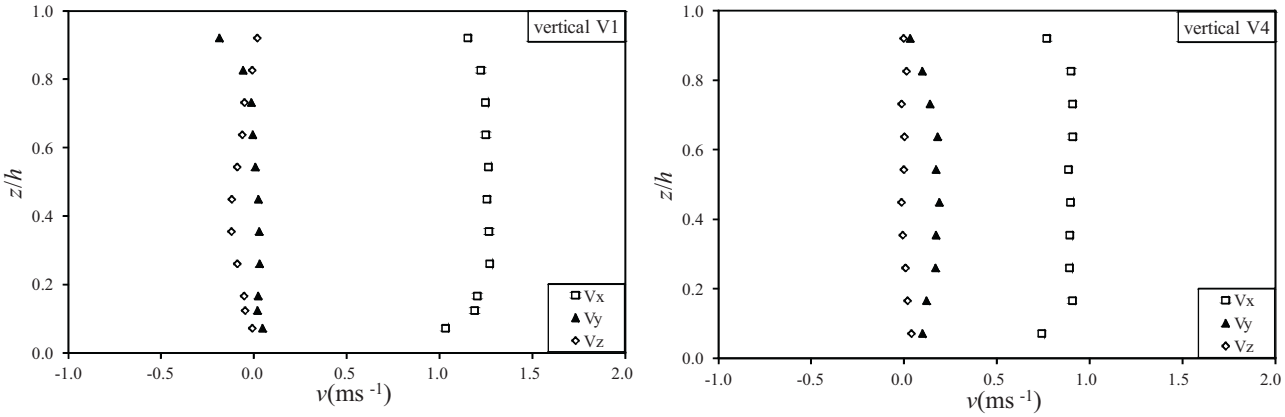

Fig. 3. Measured velocities prove the two-dimensional nature of the VSF flow.

$$\frac{\partial(hv_x)}{\partial t}+\frac{\partial(hv_x^2)}{\partial x}+\frac{\partial(hv_xv_y)}{\partial y}=-gh\frac{\partial h}{\partial x}-gh\frac{\partial z_b}{\partial x}-ghn_g^2\frac{v_x\sqrt{v_x^2+v_y^2}}{h^{4/3}}+\frac{\partial}{\partial x}\left(h\nu_T\frac{\partial v_x}{\partial x}\right)+\frac{\partial}{\partial y}\left(h\nu_T\frac{\partial v_x}{\partial y}\right) \quad (2)$$

$$\frac{\partial(hv_y)}{\partial t}+\frac{\partial(hv_xv_y)}{\partial x}+\frac{\partial(hv_y^2)}{\partial y}=-gh\frac{\partial h}{\partial y}-gh\frac{\partial z_b}{\partial y}-ghn_g^2\frac{v_y\sqrt{v_x^2+v_y^2}}{h^{4/3}}+\frac{\partial}{\partial x}\left(h\nu_T\frac{\partial v_y}{\partial x}\right)+\frac{\partial}{\partial y}\left(h\nu_T\frac{\partial v_y}{\partial y}\right) \quad (3)$$

where h is the water depth, v_x and v_y are the depth-averaged velocities in x and y direction, g is the gravity acceleration, z_b is the bed elevation level, n_g is Manning's roughness coefficient and ν_T is kinematic coefficient of eddy viscosity, determined by the appropriate turbulence model. In accordance with previous research by Bombač et al. (2014) the depth averaged $k-\varepsilon$ turbulence model of Rastogi and Rodi (1978) was used.

Numerical model of VSF consisted of 9 active pools, an inlet reach ($0.5\times L$) and an outlet reach ($3.2\times L$), where $L=3.00$ m is the length of a pool (Fig. 1). Such model dimensions ensure uniform flow past the central pools, with no potential effects of the model inlet and outlet boundary conditions (Chorda et al., 2010; Liu et al., 2006). Flow fields in adjacent central pools were compared and showed no differences. Therefore, all presented numerical results refer to the fifth (middle) pool.

A relatively dense and uniform numerical mesh was used ($\Delta x=0.01$ m; $\Delta y=0.02$ m). Such a dense mesh had to be used in order to ensure results without any significant effect of numerical diffusion (Bombač et al., 2014). To ensure numerical stability and convergence, the time step was set to $\Delta t=0.1$ s. All simulations were calculated to the final time of 3600 s.

At the inlet boundary a constant discharge with uniform velocity distribution normal to the inlet was set. A depth-discharge relation at the outlet boundary was fixed iteratively to obtain the same water depth in middle sections of central pools (uniform flow conditions). Such uniform flow conditions were also recorded during field measurements. Influence of bed friction is described by Manning's coefficient. As was shown in Bombač et al. (2014), bed friction does not play an important role for this type of flow. A more detailed description of numerical mesh analysis, effect of appropriate turbulence model and Manning's roughness coefficient can be found in Bombač et al. (2014), while a complete description of the numerical model can be found in Četina (1988) and Četina (2000).

3. Results

3.1. Measured bed and water surface elevation

Bed of the observed pool was measured at 21 points. The bed is covered with stones 0.10–0.30 m in diameter. This is in accordance with fishway design and results in bed elevation that is not completely smooth. However, measured bed elevation values indicated that the bed was level (or smooth) enough to be represented as an average of the measured values. Water surface in the observed VSF was quite undulated; its average elevation was determined on the basis of measured minimal and maximal elevations. Water surface elevation was measured in 5 cross sections located at $x=0.2$, 0.6, 1.2, 1.8 and 2.4 m, in a total of 51 points.

3.2. Measured velocity components

Flow velocities were measured in two steps. First, the measurements were conducted at various depths $z/h=0.07$, 0.17, 0.26, 0.36, 0.45, 0.54, 0.64, 0.73, 0.83 and 0.92 in 4 verticals, shown in Fig. 2 (notations V1–V4). These results showed that the flow in the observed VSF was indeed two-dimensional, i.e. the vertical component v_z was small, while horizontal components v_x and v_y remained practically constant for all z/h, as shown in Fig. 3.

Additional measurements were performed in the first step to determine the time required for the convergence of the measured values (i.e. the average of each velocity component, and of turbulent kinetic energy). With the probe located at a different point in each of the mentioned 4 verticals (one point in each V1–V4) measurements lasting up to 1222 s were performed. The results showed that sufficient convergence (±2.44%) was achieved with measurements lasting 120 s, as shown in Fig. 4. Measurements at vertical V3 are not presented, because this vertical is located near the center of the vortex and consequently the measured average values are close to 0.

On the basis of both findings from step one, velocity measurements were performed in all points shown in Fig. 2, at $z/h=0.4$ (as suggested by Maddock et al., 2013), with each measurement lasting for 120 s. Most of the measured values are collected in Tables 1–4.

Measured velocity vectors are shown in Fig. 5. This figure shows that only one larger swirling zone appears in the lower part of the pool ($y<1.3$ m). The main stream passes almost straight between

Table 1
Measured longitudinal velocity component v_x [m/s].

y [m]	x [m]														
	0.00	0.20	0.40	0.60	0.80	1.00	1.20	1.40	1.60	1.80	2.00	2.20	2.40	2.60	2.80
2.10	0.73	/	/	−0.08	−0.19	−0.06	0.02	0.27	0.35	0.47	0.64	0.77	0.86	0.90	0.93
2.00	0.84	/	/	0.13	0.03	0.12	0.23	0.32	0.52	0.61	0.72	0.83	0.91	0.96	0.95
1.90	1.01	1.47	/	0.46	0.46	0.48	0.51	0.65	0.74	0.80	0.89	0.99	0.99	1.07	1.06
1.80	1.17	1.39	1.51	1.19	1.02	0.96	0.95	1.01	1.01	1.05	1.06	1.05	1.11	1.13	1.19
1.70	1.22	1.36	1.42	1.44	1.36	1.23	1.24	1.17	1.18	1.14	1.14	1.09	1.08	1.14	1.19
1.60	1.21	1.30	1.35	1.37	1.43	1.36	1.33	1.23	1.14	1.11	1.05	0.98	1.01	1.09	1.15
1.50	1.14	1.17	1.22	1.25	1.23	1.16	1.23	1.00	1.00	0.93	0.93	0.80	0.82	1.05	1.09
1.40	/	0.89	0.95	0.98	1.03	0.97	0.94	0.84	0.77	0.68	0.66	0.61	0.48	/	/
1.30	/	0.06	0.25	0.42	0.55	0.55	0.61	0.49	0.46	0.56	0.51	0.40	0.28	/	/
1.20	/	0.01	0.05	0.13	0.23	0.32	0.33	0.37	0.29	0.30	0.32	0.27	0.25	/	/
1.10	/	−0.02	0.01	0.07	0.15	0.21	0.23	0.22	0.20	0.19	0.17	0.20	0.21	0.13	/
0.90	/	−0.07	−0.05	−0.02	0.06	0.07	0.07	0.16	0.11	0.08	0.12	0.08	0.13	0.16	/
0.70	/	−0.13	−0.14	−0.09	−0.07	0.01	−0.03	0.06	0.02	−0.01	0.00	0.01	0.02	0.04	/
0.50	/	−0.16	−0.23	−0.21	−0.16	−0.10	−0.08	−0.05	−0.11	−0.14	−0.17	−0.16	−0.11	−0.05	/
0.30	/	−0.14	−0.25	−0.29	−0.32	−0.31	−0.33	−0.31	−0.34	−0.36	−0.35	−0.31	−0.26	−0.14	/
0.13	/	−0.02	−0.07	−0.24	−0.36	−0.39	−0.45	−0.45	−0.52	−0.48	−0.41	−0.43	−0.37	−0.22	/

Table 2
Measured vertical velocity component v_y [m/s].

y [m]	x [m]														
	0.00	0.20	0.40	0.60	0.80	1.00	1.20	1.40	1.60	1.80	2.00	2.20	2.40	2.60	2.80
2.10	−0.08	/	/	−0.18	−0.07	0.01	0.00	0.12	0.09	0.14	0.16	0.17	0.17	0.16	0.13
2.00	−0.09	/	/	−0.08	−0.01	0.05	0.12	0.12	0.15	0.18	0.20	0.18	0.21	0.18	0.09
1.90	−0.06	−0.28	/	−0.01	0.07	0.12	0.14	0.23	0.22	0.23	0.25	0.26	0.24	0.21	0.11
1.80	0.03	−0.08	0.14	0.15	0.13	0.17	0.21	0.26	0.27	0.28	0.28	0.28	0.27	0.23	0.15
1.70	0.09	0.05	0.13	0.25	0.28	0.30	0.27	0.37	0.33	0.32	0.31	0.29	0.27	0.24	0.16
1.60	0.14	0.11	0.19	0.27	0.27	0.31	0.31	0.33	0.34	0.31	0.30	0.28	0.28	0.24	0.16
1.50	0.17	0.13	0.19	0.25	0.32	0.35	0.28	0.35	0.28	0.26	0.23	0.22	0.30	0.22	0.18
1.40	/	0.09	0.14	0.18	0.18	0.22	0.22	0.24	0.22	0.21	0.18	0.15	0.22	/	/
1.30	/	0.08	0.08	0.10	0.15	0.18	0.18	0.22	0.18	0.15	0.12	0.08	−0.03	/	/
1.20	/	0.08	0.10	0.12	0.14	0.16	0.16	0.15	0.13	0.12	0.08	0.01	−0.18	/	/
1.10	/	0.10	0.10	0.11	0.14	0.16	0.14	0.12	0.12	0.08	0.04	−0.06	−0.23	−0.12	/
0.90	/	0.09	0.14	0.15	0.14	0.13	0.09	0.08	0.04	0.04	−0.02	−0.10	−0.25	−0.30	/
0.70	/	0.02	0.04	0.17	0.15	0.07	0.09	0.04	0.03	−0.02	−0.07	−0.13	−0.25	−0.32	/
0.50	/	/	/	0.15	0.09	0.07	0.02	−0.01	−0.03	−0.07	−0.12	−0.17	−0.24	−0.30	/
0.30	/	/	/	0.08	0.08	0.04	0.02	−0.04	−0.07	−0.08	−0.12	−0.15	−0.19	−0.25	/
0.13	/	/	/	0.01	0.02	−0.01	0.00	−0.06	−0.06	−0.06	−0.10	−0.10	−0.14	−0.19	/

the two slots with little energy dissipation (i.e. reduction of velocity is small).

One of the important characteristics of the velocity filed is the mean flow kinetic energy per unit mass k, which is defined as:

$$k = \frac{1}{2}(v_x^2 + v_y^2 + v_z^2) \quad (4)$$

where v_x, v_y and v_z are mean longitudinal, transverse and vertical velocities, respectively. Contours of $k^{0.5}$ normalized by maximum measured velocity v_{max} are shown in Fig. 6. It can be seen that the maximum values of mean flow kinetic energy k are in the slot region ($k_{max}^{0.5}/v_{max} = 0.76$) and decrease downstream. In the swirling zone ($y < 1.3$ m), mean flow kinetic energy is low ($k^{0.5}/v_{max} < 0.10$). In an effective fishway there must be an area with low k values, where

Table 3
Measured transverse velocity component v_z [m/s].

y [m]	x [m]														
	0.00	0.20	0.40	0.60	0.80	1.00	1.20	1.40	1.60	1.80	2.00	2.20	2.40	2.60	2.80
2.10	0.06	/	/	0.03	0.13	0.19	0.17	0.19	0.14	0.14	0.17	0.12	0.10	0.08	0.06
2.00	0.02	/	/	−0.15	−0.09	−0.03	0.00	0.03	0.02	0.03	0.01	0.03	0.03	0.01	−0.01
1.90	−0.06	0.03	/	−0.15	−0.11	−0.09	−0.07	−0.04	−0.03	−0.01	−0.04	−0.03	−0.04	−0.05	−0.07
1.80	−0.12	−0.09	−0.03	−0.09	−0.10	−0.11	−0.07	−0.06	−0.09	−0.07	−0.07	−0.05	−0.05	−0.07	−0.09
1.70	−0.13	−0.14	−0.14	−0.12	−0.09	−0.11	−0.12	−0.08	−0.10	−0.08	−0.08	−0.07	−0.06	−0.07	−0.12
1.60	−0.14	−0.14	−0.15	−0.15	−0.12	−0.10	−0.13	−0.11	−0.09	−0.08	−0.06	−0.05	−0.06	−0.06	−0.09
1.50	−0.16	−0.11	−0.14	−0.13	−0.12	−0.12	−0.12	−0.07	−0.06	−0.06	−0.04	−0.03	−0.03	−0.04	−0.05
1.40	/	−0.06	−0.10	−0.14	−0.10	−0.10	−0.08	−0.04	−0.03	−0.01	−0.01	−0.01	0.01	/	/
1.30	/	−0.09	−0.09	−0.07	−0.05	−0.02	−0.02	0.00	0.02	−0.01	0.01	−0.01	0.06	/	/
1.20	/	−0.08	−0.03	0.00	0.05	0.05	0.04	0.04	0.05	0.03	0.01	−0.01	0.01	/	/
1.10	/	−0.02	0.02	0.05	0.06	0.07	0.07	0.01	0.05	0.00	−0.01	−0.02	0.00	0.01	/
0.90	/	−0.01	0.08	0.08	0.09	0.05	0.07	−0.04	−0.01	−0.02	−0.03	−0.02	−0.03	−0.03	/
0.70	/	−0.07	0.04	0.08	0.06	0.01	0.05	−0.03	−0.01	−0.02	−0.02	−0.02	−0.02	−0.02	/
0.50	/	/	/	0.08	0.06	0.00	0.03	0.02	0.03	0.02	0.03	0.00	−0.01	−0.02	/
0.30	/	/	/	0.08	0.04	0.03	0.04	0.05	0.07	0.06	0.00	0.01	−0.01	−0.07	/
0.13	/	/	/	0.03	0.00	−0.02	−0.03	0.00	−0.03	−0.05	0.02	−0.06	−0.09	−0.14	/

Table 4
Measured turbulent kinetic energy per unit mass k' multiplied by 100 [$m^2\ s^{-12}$].

y [m]	x [m]														
	0.00	0.20	0.40	0.60	0.80	1.00	1.20	1.40	1.60	1.80	2.00	2.20	2.40	2.60	2.80
2.10	6.02	/	/	5.79	7.27	9.91	10.33	11.38	11.95	10.27	9.42	9.02	7.45	7.06	6.15
2.00	6.51	/	/	9.79	10.81	12.75	13.62	13.45	13.78	11.64	11.14	9.37	8.07	7.35	7.17
1.90	6.74	6.49	/	15.88	17.19	15.72	16.31	11.98	11.39	11.06	9.77	7.99	7.69	6.66	6.55
1.80	5.64	5.89	6.36	13.47	14.39	14.39	13.36	9.91	9.86	8.51	7.17	7.29	6.27	6.17	5.80
1.70	5.14	4.96	4.84	4.64	5.71	6.85	7.35	6.36	6.42	6.30	5.86	6.53	6.28	5.86	5.58
1.60	5.18	4.69	3.89	3.76	3.66	4.08	4.60	5.94	7.22	6.49	7.53	6.96	6.24	6.17	5.96
1.50	5.44	4.82	4.23	4.04	4.53	5.69	6.14	7.77	8.12	7.99	8.35	7.38	7.37	6.03	6.18
1.40	/	6.40	6.28	7.02	7.26	8.63	8.97	8.63	8.77	8.16	7.97	7.09	7.34	/	/
1.30	/	1.02	3.64	5.71	7.58	6.25	7.79	5.80	5.52	6.05	5.76	5.60	8.01	/	/
1.20	/	0.83	1.37	1.97	2.76	3.77	3.75	2.92	3.92	3.10	4.06	4.36	7.64	/	/
1.10	/	1.11	1.21	1.16	1.71	1.64	1.97	1.51	2.27	2.17	2.51	4.01	5.72	7.80	/
0.90	/	1.35	1.54	1.37	1.19	1.43	1.43	1.08	1.54	1.35	1.31	1.96	3.79	6.53	/
0.70	/	1.45	1.69	1.22	1.22	1.07	1.48	0.96	1.36	1.57	1.43	1.32	3.00	4.36	/
0.50	/	/	/	1.40	1.39	1.26	1.31	1.46	1.27	1.10	1.29	1.63	2.59	3.14	/
0.30	/	/	/	1.35	1.24	1.25	1.47	1.32	1.66	1.30	1.25	1.78	2.09	2.65	/
0.13	/	/	/	1.36	1.04	1.29	1.24	1.32	1.60	1.29	1.47	1.91	1.93	2.49	/

fish can rest, and the area with high k values should preferably be small (Liu et al., 2006).

3.3. Measured turbulent kinetic energy

As already stated in previous works by Calluaud et al. (2014), Chorda et al. (2010), Liu et al. (2006), Tarrade et al. (2011), turbulence characteristics must be taken into account in the process of dimensioning a fishway. Therefore, turbulent kinetic energy per unit mass k' was calculated from the velocity measurements:

$$k' = \frac{1}{2}(\bar{v}_x'^2 + \bar{v}_y'^2 + \bar{v}_y'^2) \quad (5)$$

where v_x', v_y', v_z' are longitudinal, transverse and vertical velocity fluctuations, respectively. Fig. 7 shows the contours of the square root of turbulent kinetic energy per unit mass k' normalized by maximum velocity v_{max}. It can be seen that values of $k'^{0.5}$ are relatively small compared to v_{max} ($k'^{0.5}/v_{max} = 0.131$). Maximum values of the square root of k' were measured downstream of the smaller baffle and did not exceed 30.3% of v_{max}. Lower values of k' in fishways are preferred as fish avoid entering areas with excessively high turbulence intensity (Bell, 1990).

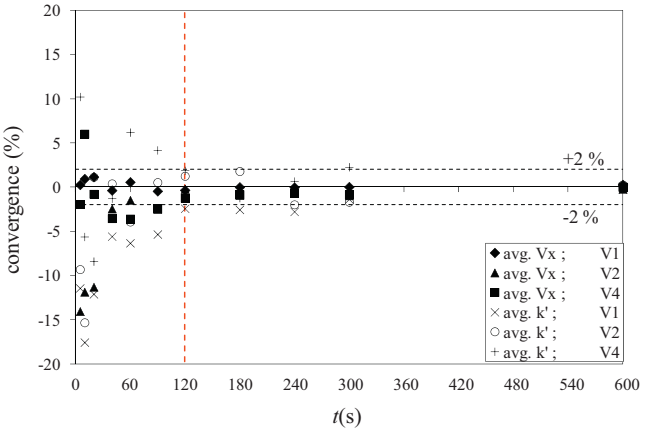

Fig. 4. The convergence of the measured longitudinal velocity component v_x and turbulent kinetic energy per unit mass k', both at locations V1–V4.

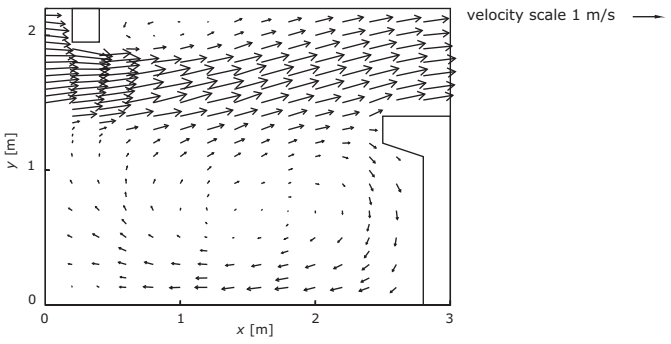

Fig. 5. Measured velocity vectors in the central pool of VSF Arto – Blanca at $z/h = 0.4$.

3.4. Results of numerical simulations

Simulations of flow in VSF were performed with the same hydraulic parameters as were maintained during field measurements. Boundary conditions were set up as described in Section 2.2. Uniform flow conditions (the same water depth in comparable points in the middle pools of the VSF) were ensured. Manning's roughness coefficient $n_g = 0.030\ s\ m^{-1/3}$ was selected

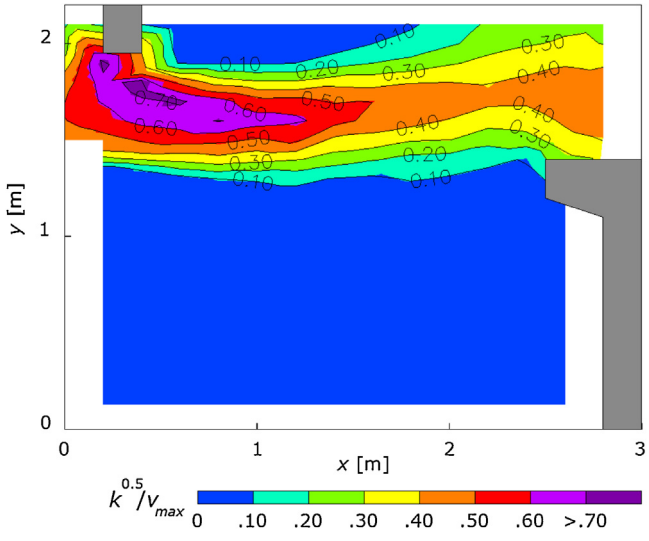

Fig. 6. Square root of mean flow kinetic energy per unit mass k normalized by maximum measured velocity v_{max}.

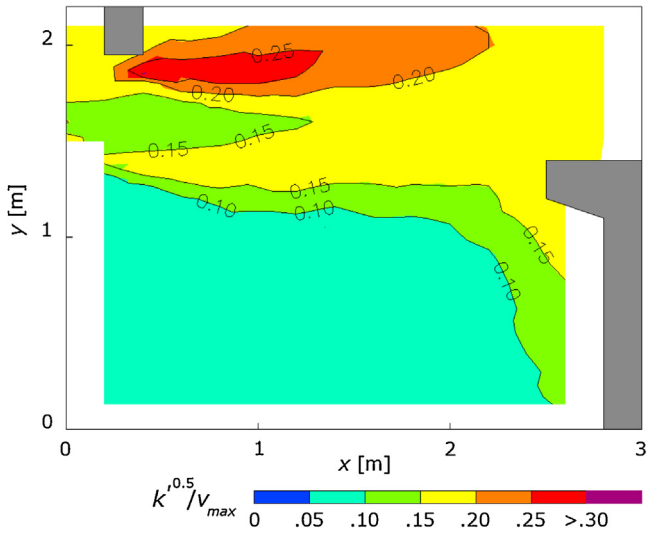

Fig. 7. Square root of turbulent kinetic energy per unit mass k' normalized by maximum measured velocity v_{max}.

according to the fishway bed material. As shown in Bombač et al. (2014), bed friction does not play an important role for this type of flow, thus no special calibration of the PCFLOW2D model was needed.

Results from the numerical model PCFLOW2D can easily be presented in numerous ways. Figs. 8 and 9 show calculated isovels, dimensionless streamlines ψ', turbulent kinetic energy per unit mass k' and dissipation of turbulent kinetic energy per unit mass ε which is expressed as:

$$\varepsilon = \frac{k'^{3/2}}{l} \tag{6}$$

where l is the dissipation length. The dimensionless value of the streamline is defined as:

$$\psi' = \frac{\psi}{Q} \tag{7}$$

where ψ is the dimensional value of the streamline and Q is the discharge in the fishway.

4. Discussion

4.1. Two-dimensional nature of the VSF flow

Measured vertical velocities v_z are negligibly small in comparison to longitudinal velocities v_x. Both horizontal velocities remain practically constant with depth. This means that depth-averaged 2D models can be employed to simulate VSF fishways with geometrical and flow properties similar to the observed one. This confirms the findings by Cea et al. (2007), Chorda et al. (2010), Puertas et al. (2012) and Violeau (2012).

4.2. Required duration of measurements

In a given point the average values of measured velocity components and of their fluctuations (turbulent kinetic energy) remained practically constant after 120 s of measurement. This

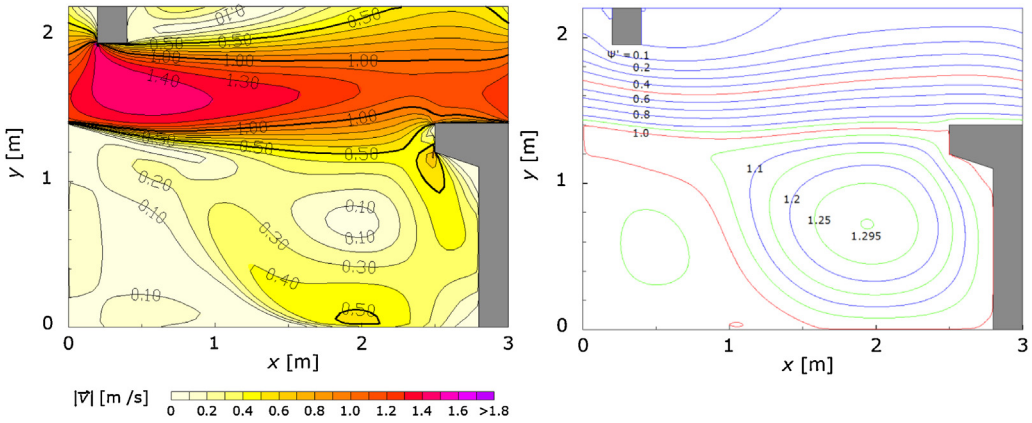

Fig. 8. Calculated isovels (left); calculated dimensionless streamlines ψ' in the middle pool of the fishway (right).

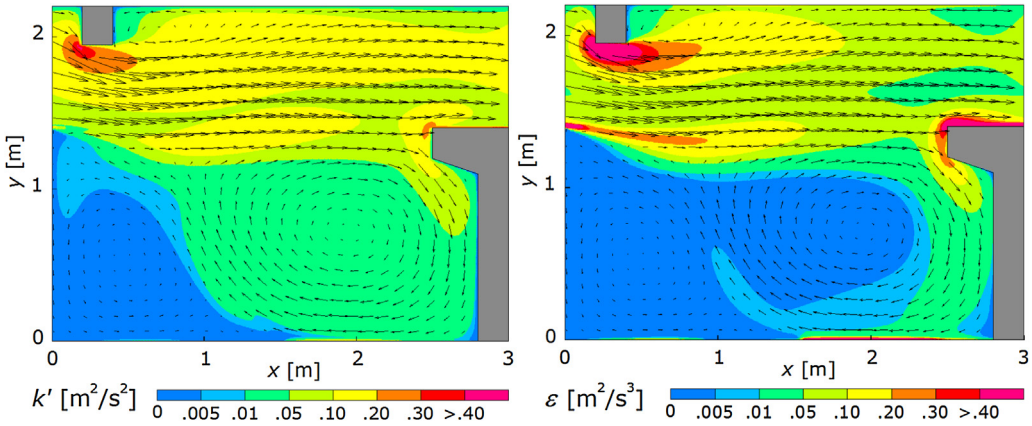

Fig. 9. Turbulent kinetic energy per unit mass k' [$m^2\ s^{-2}$] (left); dissipation of the turbulent kinetic energy per unit mass ε [$m^2\ s^{-3}$] (right).

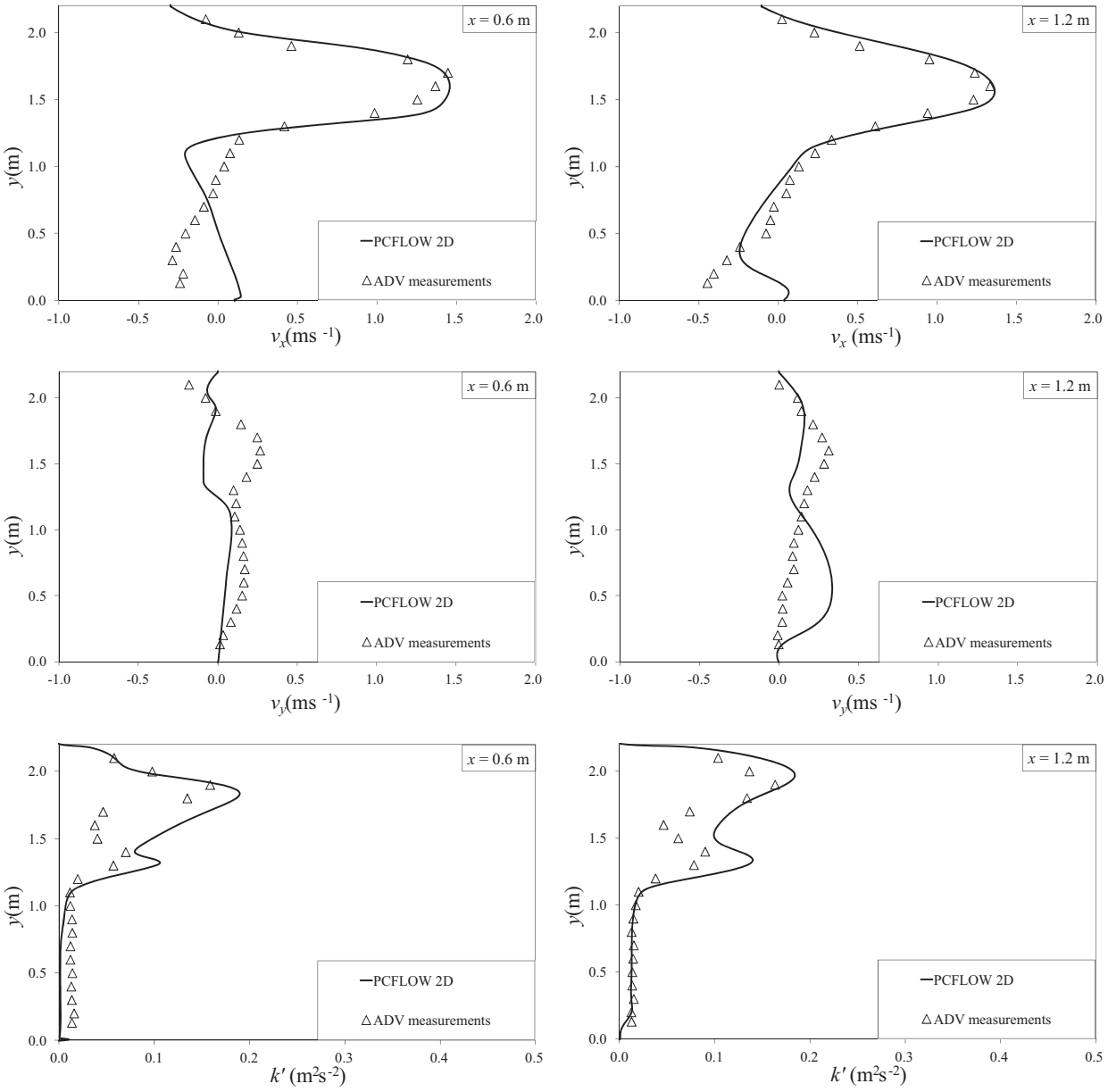

Fig. 10. Calculated and measured velocity components v_x and v_y, and turbulent kinetic energy per unit mass k' at cross sections $x = 0.6$ and 1.2 m.

means that for accurate determination of the velocity field in the VSF pool, measurements that are longer than 15 s (Puertas et al., 2004), 60 s (Yagci and Kabdasli, 2008), 30 or 90 s (Santos et al., 2012), but shorter than 300 or 600 s (Liu et al., 2006) are required. Regarding the convergence time of the results the present study is in accordance with Calluaud et al. (2014).

4.3. Maximum velocities

Measured longitudinal velocity components v_x reached 1.5 m/s. As pointed out in the introduction, some recent references on fishway design state that for the discussed VSF geometry ($\Delta h = 0.05$ m) maximum flow velocity is or should be about 1 m/s according to relation $v_{max} = (2g\Delta h)^{1/2}$. This is 50% smaller than values measured in the presented VSF. It should be pointed out that the relation $v_{max} = (2g\Delta h)^{1/2}$ is an approximation, which stands "if the velocity in the upstream pool is neglected" (Bermúdez et al., 2010, p. 1360). In the presented VSF such a criterion is unrealistic. With actual maximum velocities being considerably larger than values resulting from $v_{max} = (2g\Delta h)^{1/2}$, several problems arise. Firstly, the VSF should be designed to provide upstream migration even for the weakest swimmers, but this is not achieved. Secondly, the discharge in the VSF is 50% larger, which is uneconomical. Thirdly, as a consequence, some other elements of the fishway are also non-optimal (e.g. intake, natural-like reach, outflow).

4.4. Evaluation of the PCFLOW2D numerical model

Calculated water depths were in accordance with the measured ones. In Figs. 10 and 11, the calculated velocity components v_x and v_y and calculated turbulent kinetic energy per unit mass k' are compared with the measured values.

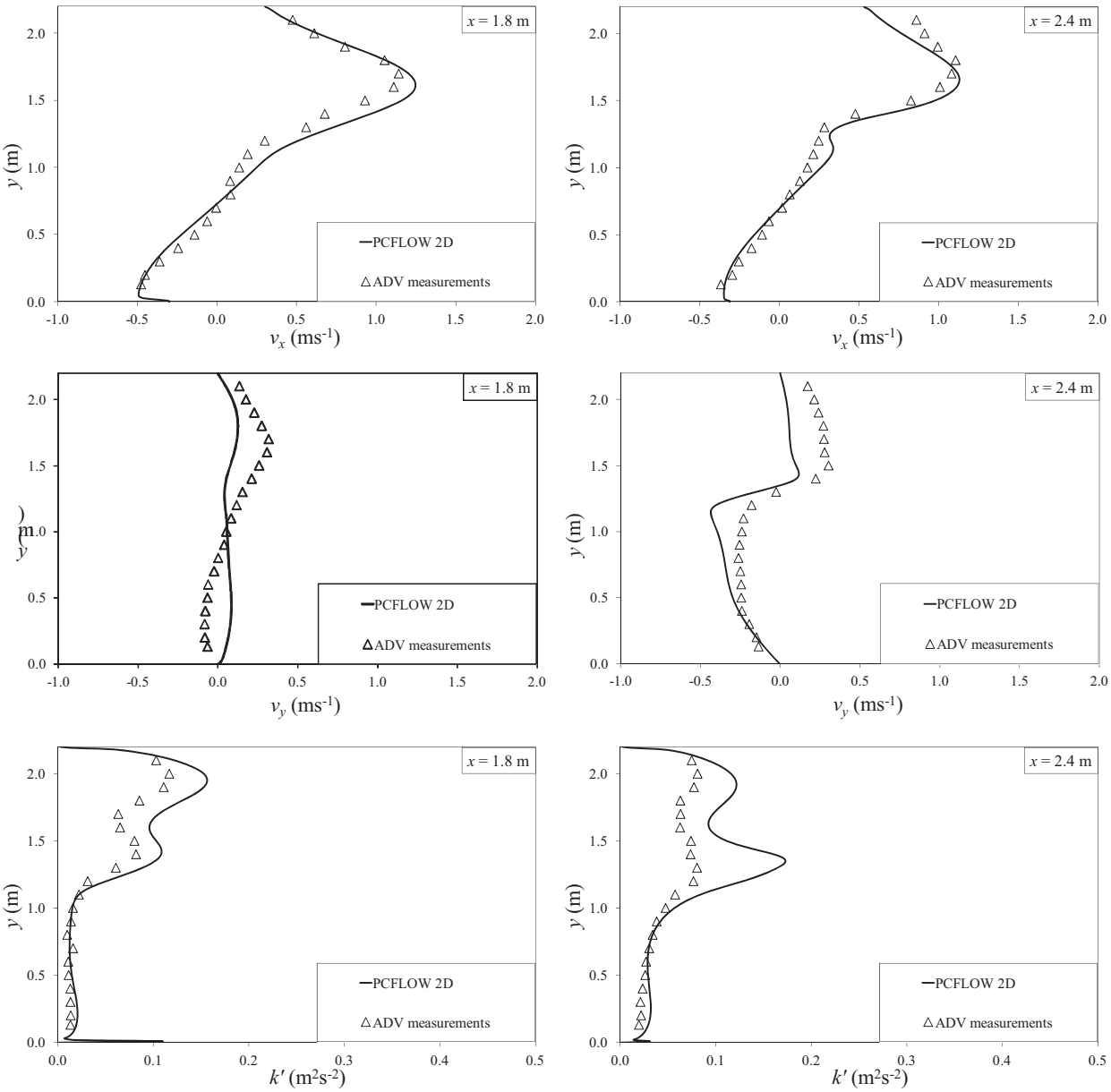

Fig. 11. Calculated and measured velocity components v_x and v_y, and turbulent kinetic energy per unit mass k' at cross sections $x = 1.8$ and 2.4 m.

Comparison of results shown in Figs. 10 and 11 demonstrates that PCFLOW2D is a reliable tool for accurate simulations of VSF flow and can therefore be used for the optimization of such fishways. A correct and detailed simulation of the flow field in a fishway is of great importance especially in the light of the equation for v_{max} found in design manuals, which seems to be based on a somewhat unrealistic criterion.

4.5. Energy dissipation

Another important flow parameter in VSF design is the energy dissipation rate per unit volume E. Lower values are generally preferred. For fishways designed for riverine species, such as the VSF Arto – Blanca, the average energy dissipation rate per unit volume $\bar{E}$ of less than 200 W/m^3 is advisable (Larinier, 2002). However, detailed determination of spatial distribution of the energy dissipation rate is of great importance for better evaluation of fish ability to pass through the VSF (Chorda et al., 2010). Average value of E in the pools is usually calculated using a simplified formula:

$$\bar{E} = \frac{\rho g Q \Delta h}{V_p} \tag{8}$$

where ρ is the water density and V_p is the pool water volume. In our case Eq. (8) gives $\bar{E} = 58$ W/m^3. PCFLOW2D allows E to be calculated as $\rho \times \varepsilon$, and integration gave $\bar{E} = 64$ W/m^3 in the central pool. The agreement of results is similar to the one presented by Chorda et al. (2010). Contours of calculated E normalized by $\bar{E} = 64$ W/m^3 are shown in Fig. 12.

As can be seen from Fig. 12, the dissipation rate is much higher in the slot region and especially near the small baffle. Nevertheless, the energy dissipation rate E exceeded the recommended average value of 200 W/m^3 only in 3.7% of the pool area. We can therefore conclude that the present VSF is very fish-friendly in terms of energy dissipation rate.

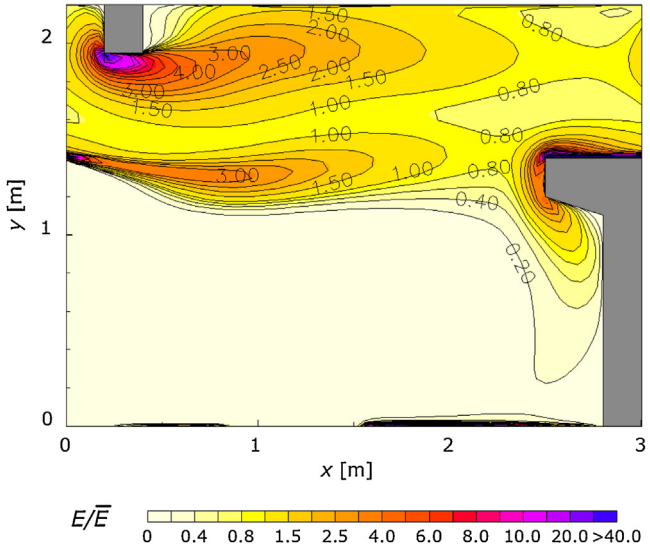

Fig. 12. Dissipation rate E normalized by average dissipation rate $\bar{E}$.

5. Conclusions

Extensive field measurements and numerical simulations of the flow in an operational VSF at Arto – Blanca hydropower plant allow us to draw the following conclusions:

1) Measured velocities in the vertical direction are negligibly small, while the horizontal velocities remain practically constant with depth. This means that depth-averaged 2D numerical models can be employed to simulate vertical slot fishways with geometrical and flow properties similar to the presented one. This confirms the findings by Cea et al. (2007), Chorda et al. (2010), Puertas et al. (2012) and Violeau (2012).
2) The average values of measured velocity components and of their fluctuations (turbulent kinetic energy) at a given point remain practically constant after 120 s of the measurement.
3) Maximum flow velocity values calculated from the relation $v_{max} = (2g\Delta h)^{1/2}$, as suggested in some manuals for fishway design, can be up to 50% smaller than those measured in the studied VSF. The mentioned v_{max} equation seems to be based on a somewhat unrealistic assumption. We believe that in a process of VSF design numerical simulations, such as those with PCFLOW2D, should be used instead of over-simplified relations such as the one mentioned above.
4) PCFLOW2D allowed exact calculation of energy dissipation and these results proved to be similar to ones presented by Chorda et al. (2010). Calculated energy dissipation values were below the recommended limit, thus indicating that the present VSF was very fish-friendly (in terms of energy dissipation rate) – as was indeed confirmed with the field monitoring of the prototype VSF.
5) PCFLOW2D model proved to be a reliable tool for accurate simulations and optimizations of vertical slot fishways.

References

Bell, M.C., 1990. Fisheries Handbook of Engineering Requirements and Biological Criteria. U.S. Army Corps of Engineers, North Pacific Division, Portland, OR, pp. 353.

Bermúdez, M., Puertas, J., Cea, L., Pena, L., Balairón, L., 2010. Influence of pool geometry on the biological efficiency of vertical slot fishways. Ecol. Eng. 36 (10), 1355–1364, http://dx.doi.org/10.1016/j.ecoleng.2010.06.013.

Bombač, M., Novak, G., Rodič, P., Četina, M., 2014. Numerical and physical model study of a vertical slot fishway. J. Hydrol. Hydromech. 62 (2), 1–10, http://dx.doi.org/10.2478/johh-2014-0013.

Calluaud, D., Pineau, G., Texier, A., David, L., 2014. Modification of vertical slot fishway flow with a supplementary cylinder. J. Hydraul. Res. 52 (5), 614–629, http://dx.doi.org/10.1080/00221686.2014.906000.

Cea, L., Pena, L., Puertas, J., Vazquez-Cendon, M.E., Pena, E., 2007. Application of several depth-averaged turbulence models to simulate flow in vertical slot fishways. J. Hydraul. Eng. 133 (2), 160–172, http://dx.doi.org/10.1061/(ASCE)0733-9429(2007)133:2(160).

Chorda, J., Maubourguet, M.M., Roux, H., George, J., Larinier, M., Tarrade, L., David, L., 2010. Two-dimensional free surface flow numerical model for vertical slot fishways. J. Hydraul. Res. 48 (2), 141–151, http://dx.doi.org/10.1080/00221681003703956.

Ciuha, D., Povž, M., Kvaternik, K., Brenčič, M., Muck, P., 2014. The design and technical solutions of passages for aquatic organisms at the HPP on the lower Sava River reach, with an emphasis on the passage at HPP Arto – Blanca. Mišič's Water Manag. day 25, 228–236 (in Slovenian). Available from: http://www.mvd20.com/LETO2014/R34.pdf.

Četina, M., 1988. Mathematical modeling of two-dimensional turbulent flows. Acta Hydrotech. 6 (5), 1–56 (in Slovenian with extended abstract in English).

Četina, M., 2000. Two-dimensional modeling of free surface flow. Acta Hydratech. 18 (29), 23–37 ftp://ksh.fgg.uni-lj.si/acta/a29-mc.pdf.

Katopodis, C., 1992. Introduction to Fishway Design. Working Doc. Freshwater Institute, Winnipeg, Canada, pp. 70.

Kolman, G., Mikoš, M., Povž, M., 2010. Fish passages on hydroelectric power dams in Slovenia. Nat. Conserv. 24, 85–96 (in Slovenian). Available from: http://www.zrsvn.si/dokumenti/63/2/2010/Kolman_Mikos_povz_2227.pdf.

Larinier, M., 2002. Pool fishways, pre-barrages and natural bypass channels. In: Larinier, M., Travade, F., Porcher, J.P. (Eds.), Fishways: Biological Basis, Design Criteria and Monitoring, vol. 364, Suppl, pp. 54–82.

Liu, M., Rajaratnam, N., Zhu, D.Z., 2006. Mean flow and turbulence structure in vertical slot fishways. J. Hydraul. Eng. 132 (8), 765–777, http://dx.doi.org/10.1061/(ASCE)0733-9429(2006)132:8(765).

Maddock, I.P., Harby, A., Kemp, P., Wood, P. (Eds.), 2013. Ecohydraulics: An Integrated Approach. Wiley-Blackwell, p. 446.

Marriner, B.A., Baki, A.B.M., Zhu, D.Z., Thiem, J.D., Cooke, S.J., Katopodis, C., 2014. Field and numerical assessment of turning pool hydraulics in a vertical slot fishway. Ecol. Eng. 63, 88–101, http://dx.doi.org/10.1016/j.ecoleng.2013.12.010.

Puertas, J., Pena, L., Teijeiro, T., 2004. Experimental approach to the hydraulics of vertical slot fishways. J. Hydraul. Eng. 130 (1), 10–23, http://dx.doi.org/10.1061/(ASCE)0733-9429(2004)130:1(10).

Puertas, J., Cea, L., Bermúdez, M., Pena, L., Rodríguez, A., Rabuñal, J.R., Balairón, L., Lara, Á., Aramburu, E., 2012. Computer application for the analysis and design of vertical slot fishways in accordance with the requirements of the target species. Ecol. Eng. 48, 51–61, http://dx.doi.org/10.1016/j.ecoleng.2011.05.009.

Rajaratnam, N., Van der Vinne, G., Katopodis, C., 1986. Hydraulics of vertical slot fishways. J. Hydraul. Eng. 112 (10), 909–927, http://dx.doi.org/10.1061/(ASCE)0733-9429(1986)112:10(909).

Rajaratnam, N., Katopodis, C., Solanki, S., 1992. New designs for vertical slot fishways. Can. J. Civil Eng. 19 (3), 402–414, http://dx.doi.org/10.1139/l92-049.

Rastogi, A.K., Rodi, W., 1978. Predictions of heat and mass transfer in open channels. J. Hydraul. Div. 104 (3), 397–420.

Santos, J.M., Silva, A., Katopodis, C., Pinheiro, P., Pinheiro, A., Bochechas, J., Ferreira, M.T., 2012. Ecohydraulics of pool-type fishways: getting past the barriers. Ecol. Eng. 48, 38–50, http://dx.doi.org/10.1016/j.ecoleng.2011.03.006.

Tarrade, L., Texier, A., David, L., Larinier, M., 2008. Topologies and measurements of turbulent flow in vertical slot fishways. Hydrobiology 609, 177–188, http://dx.doi.org/10.1007/s10750-008-9416-y.

Tarrade, L., Pineau, G., Calluaud, D., Texier, A., David, L., Larinier, M., 2011. Detailed experimental study of hydrodynamic turbulent flows generated in vertical slot fishways. Environ. Fluid Mech. 11, 1–21, http://dx.doi.org/10.1007/s10652-010-9198-4.

The Habitat Directive – FFH, Directive 92/43/EEC. Available from: http://eur-lex.europa.eu/legal-content/EN/TXT/?uri=CELEX:31992L0043.

Violeau, D., 2012. Fluid Mechanics and the SPH Method: Theory and Applications, First ed. Oxford, United Kingdom.

Yagci, O., Kabdasli, M.S., 2008. The impact of different forms of single natural vegetation elements on flow characteristics in open channels. Hydrol. Process. 22 (21), 4310–4321, http://dx.doi.org/10.1002/hyp.7018.

Water Framework Directive 2000/60/EC. Available from: http://eur-lex.europa.eu/legal-content/EN/TXT/?uri=CELEX:32000L0060.